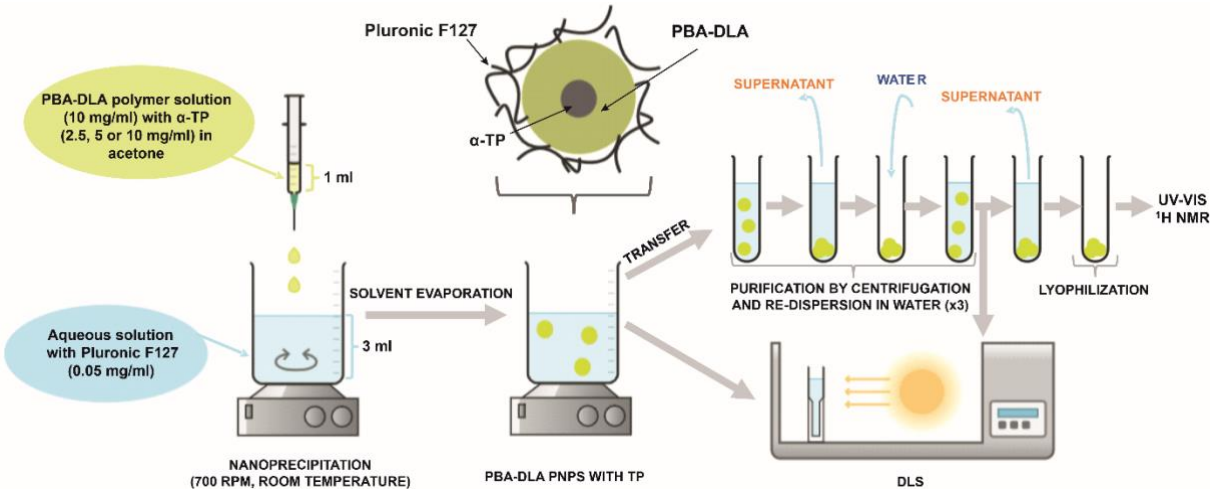

Vitamin E-loaded polymeric nanoparticles from biocompatible adipate-based copolymer obtained using the nanoprecipitation method

Martyna Sokołowska, Maja Marchwiana, Miroslawa El Fray*

West Pomeranian University of Technology, Szczecin, Faculty of Chemical Technology and Engineering, Department of Polymer and Biomaterials Science, Al. Piastow 45, 71-311 Szczecin, Poland

*Corresponding author: mirfray@zut.edu.pl

Abstract

Despite the search for new biomaterials dedicated for biomedical applications intensified in recent decades, this field is still not fully explored. Therefore, the synthesis of novel aliphatic biopolyesters poly(butylene adipate-co-dilinoleic adipate) (PBA-DLA) was performed using monomers derived from natural sources and enzyme lipase B *Candida antarctica* (CALB) as biocatalyst in order to provide fully biobased and biodegradable material suitable for drug delivery systems. Proton nuclear magnetic spectroscopy (^{1}H NMR) analysis confirmed chemical structure of PBA-DLA copolyester whereas *in vitro* cytotoxicity assay indicate on material biocompatibility. By applying a single-step nanoprecipitation method narrowly distributed PBA-DLA nanoparticles (NPs) with hydrodynamic diameter (HD) of ~200 nm were produced, however, after purification (centrifugation) step NPs tend to agglomerate. In order to eliminate this drawback suitable amount of stabilizer (Pluronic F127, 0.05 mg/ml) was selected and NPs with HD of ~149 nm were obtained. The PBA-DLA NPs could be loaded with the hydrophobic α-tocopherol (α-TP) – main ingredient of vitamin E, with encapsulation efficiency ranging from 48 to 74 % depending on tested α-TP concentration (2.5, 5, 10 mg/ml) as evidenced by combined dynamic light scattering (DLS), ultraviolet-visible spectroscopy (UV-VIS) and ^{1}H NMR measurements.

Keywords: poly(butylene adipate), enzymatic synthesis, CALB, block copolymers, polycondensation, nanoprecipitation, vitamin E.

1. Introduction

It is well known that polymeric nanoparticles (PNPs) show outstanding potential as a useful element in advanced materials science with a myriad of applications in many fields such as biotechnology, environmental technology, and especially biomedicine including anticancer therapies [1], vaccines [2], gene delivery [3], diagnostic [4], and nanopharmacy [5]. This wide range of possible applications can be covered due to the physical properties of polymers which can be frequently and easily tuned to meet certain requirements. The advantages of using polymeric materials as drug carriers are increased protection of therapeutic substances from degradation, sustained and controlled drug release depending on the degradation profile of the polymer, high cellular internalization, and ability to deliver drugs across a range of biological barriers [6–8].

There is an extensive library of biodegradable polymers available for NPs preparation whereas the vast majority belong to the family of polyesters, including poly(lactide) (PLA), poly(ε-caprolactone)(PCL), poly(trimethylene-carbonate) (PTMC), etc. [9,10]. Block copolyesters are also known as drug carriers since copolymerization is a very beneficial tool that can remarkably change the material hydrophilicity. In this context, copolymers of PLA with glycolic acid (i.e., poly(lactic-co-glycolic acid), PLGA) were probably the most widely explored and they are already commercially available [11–14]. However, despite their indisputable advantages, PLA and PLGA-based drug delivery systems also face a number of challenges such as initial burst release, incomplete drug dissolution, and enhanced lag time [13,14]. Considering those facts, new types of biodegradable polyesters need to be proposed to overcome these limitations. Poly(butylene adipate) (PBA) aliphatic polyester is mainly used in industrial applications, for example as a building block of poly(butylene adipate-co-terephthalate) (PBAT) commercially known as Ecoflex® (BASF), which is marketed as fully biodegradable plastic [15]. Interestingly enough, PBA copolymerization with different comonomers also led to novel biomedical materials showing both biodegradability and good biocompatibility. They were already evaluated as drug delivery systems [16] and performed *in vitro* release studies indicated controlled release patterns connected with both drug diffusion and polymer degradation, where the degradation profile was moderated by PBA content within copolymer structure. Other interesting components for the preparation of biodegradable PNPs are fatty acids (FA) as hydrophobic compounds naturally occurring in the human body which may retain hydrophobic drugs due to hydrophobic interactions. Dilinoleic diol (DLD) is a compound obtained *via* the dimerization process of linoleic/oleic fatty acids [17] which is suitable for step-growth polycondensation since its encapped with two functional groups. Block

copolymers based on DLD monomer have already been proposed in the literature as materials with potential use in many biomedical applications, including bone and tissue engineering or drug delivery systems but using poly(butylene succinate) (PBS) instead of PBA [18–21].

Inspired by those facts, we designed novel poly(butylene adipate-*co*-dilinoleic adipate) (PBA-DLA) block copolymer using enzyme lipase B from *Candida antarctica* (CALB) as biocatalyst to obtain fully biobased material since both monomers and catalyst are derived from natural sources. Enzymatic catalyst due to its high stereo-, enantio-, and regioselectivity can provide materials with a highly ordered structure which is a desirable feature, especially in the pharmaceutical industry. Immobilized form of CALB facilitates its easy removal after the synthesis and therefore no catalyst residues are remaining in the material matrix, which is very common drawback regarding metal-based catalysts [22]. Furthermore, the results of the α-TP-loaded nanocomposites using PBA-DLA as a carrier have been accomplished and the decisive role of a drug concentration on the NPs size and encapsulation efficiency has been investigated.

2. Materials and Methods

2.1 Materials

The following chemicals were purchased from Sigma-Aldrich: α-tocopherol (α-TP, ≥97%), diphenyl ether (DE; ≥99%), mouse fibroblasts L929 EACC, Dulbecco's Modified Eagle's Medium (DMEM), Dulbecco's Phosphate Buffered Saline (DPBS), resazurin, penicillin, streptomycin, bovine fetal serum (FBS), L-glutamine. Diethyl adipate (DA; ≥99%) was ordered from Matrix Chemicals (Sevelen, Switzerland). 1,4-butanediol (BD; ≥99%) was ordered from Alfa Aesar (Kandel, Germany). Dimer linoleic diol (DLD; ≥96.5%) (trade name: Pripol™ 2033) was provided by Cargill Bioindustrial (Gouda, The Netherlands). Chloroform (≥98.5%) was purchased from Chempur (Piekary Slaskie, Poland) and methanol (≥99.8%) was ordered from Stanlab (Lublin, Poland). Polycaprolactone CAPA 6430 was purchased from Perstop (Warrington, UK). 1,4-dioxane (≥99%) was acquired from POCH SA (Gliwice, Poland) and Pluronic® F127 (PLUR) was purchased from BASF (Ludwigshafen, Germany). *Candida Antarctica* lipase B (CALB) covalently immobilized on polyacrylate beads (300-500 μm; ≥95%, Fermase CALB™ 10000), with a nominal activity of 10 000 PLU/g (propyl laurate units per gram dry weight) was acquired from Fermenta Biotech Ltd, Mumbai and Enzyme Catalyzed Polymers LLC (Akron, OH, USA). CALB was pre-dried under vacuum for 24h at 40°C and diphenyl ether was stored over 4Å molecular sieves prior to use.

2.2 CALB catalyzed polycondensation in diphenyl ether

The copolyester of poly(butylene adipate)-co-(dilinoleic adipate) (PBA-DLA) with 70-30 wt% hard to soft segment ratio was synthesized *via* two-stage polycondensation method in diphenyl ether using CALB as biocatalyst. Briefly, CALB (10 wt% of total monomers), BD, DA, DLD, and diphenyl ether (200 wt% of total monomers) were added to a round bottom flask and placed into a heated oil bath on a magnetic stirrer. The first step was carried out under inert gas flow at atmospheric pressure and at an initial temperature of 80 °C. After 1 h the temperature was slowly increased to 95° C and the collection of ethanol was monitored for 3 h. Further, oligomerization was conducted under a pressure of 600 Torr for 21 h. In the next step, the pressure was gently reduced to 2 Torr, while still maintaining the reaction temperature at 95 °C for 72 h. Upon completion, the product mixture was dissolved in chloroform and filtered to remove CALB. The obtained chloroform solution was added dropwise to cold methanol under continuous stirring to precipitate a white polymer product. The precipitated product was filtered, washed three times with cold methanol, collected, and dried in vacuo at 40 °C for 24 h.

2.3 In vitro cytotoxicity

The potential cytotoxicity or growth inhibitory effect of the PBA-DLA copolyester was investigated in cell culture, using L929 mouse fibroblasts based on ISO 1993-5. Cells (passages 15-20) were kept in growth media (DMEM, 10% FBS, 2 mM L-glutamine, 100 U/ml penicillin, and 100 µg/ml streptomycin) in a T25 flask. For the experiments, a sub-confluent T25 flask of L929 cells was trypsinized and 1×10^4 cells per well were seeded in a 96-well plate. In parallel, a 100µm-thick film of PBA-DLA copolyester and reference material (polycaprolactone PCL CAPA® 6430) was cut into the three 6 cm^2 samples which were then sterilized in UV light for 15 minutes on each side. Next, samples of the material (n=3) were cut into smaller pieces and placed into a 24-well plate and 1 ml of medium was added to each well. The plates were then incubated for 24 hours (5% CO_2, 37 °C) to allow the cells to adhere and spread, after which the media was aspirated and replaced with 100 µl of growth media containing extracts from tested materials (6 technical replicates were performed per material). Sham control was prepared by giving 100 µl of pure growth media. The plate was incubated for 24 hours and then cell viability was assessed *via* an inverted light microscope (Delta Optical IB-100) and resazurin viability assay [23] using a fluorescent plate reader (Biotek Synergy HTX, excitation 540 nm, emission 590 nm). During resazurin viability assay complete growth media was added to the empty well without cells and it was considered as a blank. The obtained results were expressed as the percent of normalized cell viability (CV%) calculated using an equation [24].

$$CV\% = \frac{(FL_s - FL_b)}{(FL_c - FL_b)} \times 100\% \quad (1)$$

where FL is the fluorescence intensity and indexes *s*, *b*, and *c* refer to sample, blank, and control, respectively.

2.4 Encapsulation of vitamin E (a-tocopherol)

The α-TP-loaded PBA-DLA NPs were prepared *via* the nanoprecipitation method as shown in Figure 1. Briefly, the PBA-DLA (10 mg/ml) and α-TP with increasing concentrations (2.5, 5, and 10 mg/ml) were dissolved in 1 ml of acetone, which was dropped slowly into the aqueous solution of the PLUR stabilizer (3 ml, 0.05 mg/ml) under room temperature using magnetic stirring with 700 rpm. Next, the dispersion was centrifugated at 15000 rcf (t = 15 min, T = 4 °C). After the supernatant was removed, the NPs were redispersed in deionized water and the washing methods were repeated three times. The obtained NPs samples were frozen in -20 °C and lyophilized (Christ Alpha 1-2 LDplus apparatus).

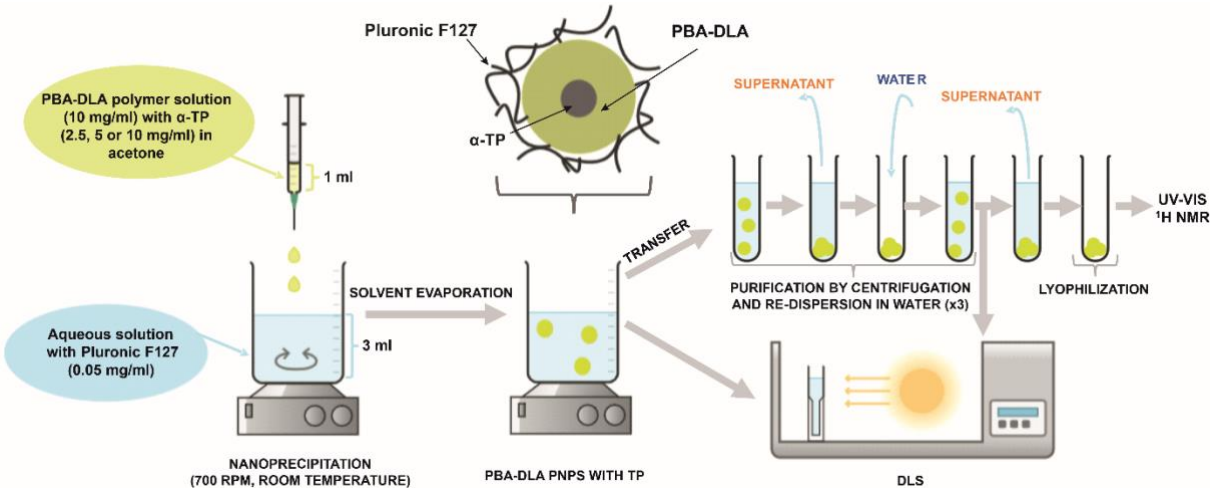

Figure 1. Schematic representation of the preparation of α-TP-loaded PBA-DLA nanoparticles stabilized with Pluronic F127 *via* nanoprecipitation method (https://chemix.org/).

2.5 Nuclear Magnetic Resonance Spectroscopy (NMR)

^{1}H NMR spectra of PBA-DLA copolyester and PBA-DLA NPs containing different concentrations of α-TP were recorded with a Bruker DPX 400 spectrometer (400 MHz, 1 s relaxation delay, 128 scans). The samples were dissolved in $CDCl_3$ and tetramethylsilane (TMS) was used as an internal reference.

2.6 Dynamic Light Scattering (DLS)

The NPs size was assessed by dynamic light scattering (DLS) using Zetasizer Nano Malvern Zen 3600 equipped with He-Ne laser (633 nm, 4 mW). The measurements were performed at 25 ± 0.1 °C with a 90° detection angle. Particle size was measured after the nanoprecipitation process and after purification steps to verify dispersion stability.

2.7 Ultraviolet-visible spectroscopy (UV-VIS)

The particles were dissolved in 1,4-dioxane to determine the encapsulation efficiency (EE%). The absorbance spectra of the prepared solutions were measured by a Jasco V-630 double-beam spectrophotometer. The spectra were registered in the range of 400–200 nm using a 1 cm quartz cuvette at room temperature. The characteristic absorbance band of the α-TP appeared at 294 nm. The concentration of the encapsulated drug was calculated based on the calibration curve. The data of the EE% was calculated from the mass of the PBA-DLA NPs following the equation (1):

$$EE\% = \frac{encapsulated\ mass\ of\ \alpha-TP}{total\ mass\ of\ the\ \alpha-TP\ in\ synthesis} \times 100\% \quad (1)$$

3. Results and discussion

Fully biobased PBA-DLA copolymer containing 70 wt% poly(butylene adipate) (PBA) as the hard segments and 30 wt% poly(dilinoleic adipate) (DLA) as the soft segments was successfully synthesized *via* two-step polycondensation in diphenyl ether using CALB as biocatalyst as presented in Figure 2. After synthesis, the material was recovered within a high reaction yield (88 %).

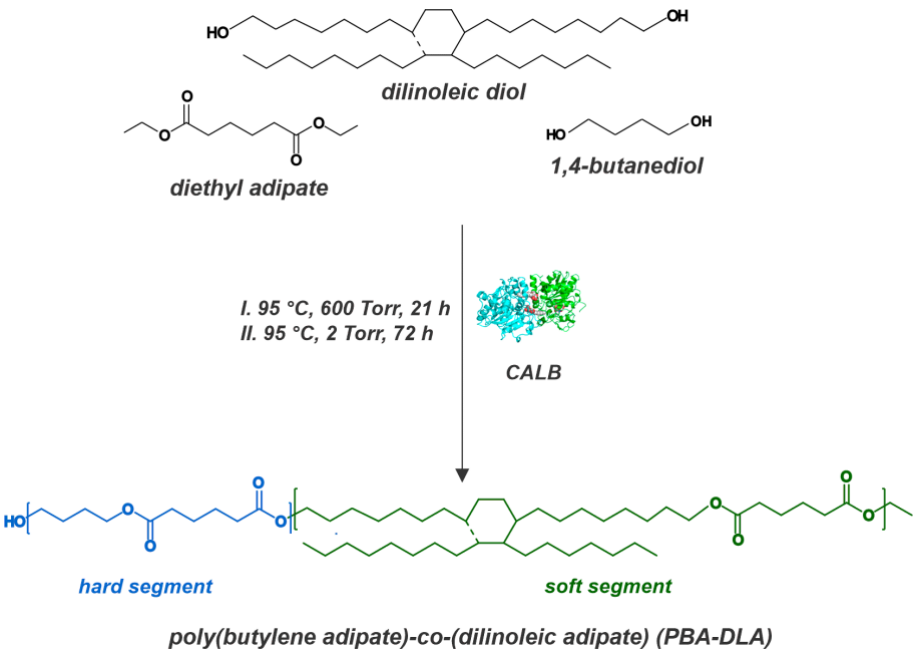

Figure 2. Synthesis of poly(butylene adipate)-co-(dilinoleic adipate) (PBA-DLA) copolymer with hard to soft segment ratio of 70-30 wt% *via* two-step polycondensation in diphenyl ether using CALB.

To confirm the chemical structure of obtained copolymer ^{1}H NMR spectra were recorded based on which detailed structural analysis was conducted. Figure 3 depicts ^{1}H NMR spectra of PBA-DLA copolyester with a 70-30 wt% hard to soft segment ratio and the detailed NMR assignments are as follows: ^{1}H NMR (400 MHz, $CDCl_3$-d_1, ppm): 4.09 (**a**) (4H, -O-C**H**$_2$, from 1,4-BDO), 4.05 (**e**) (4H, -O-C**H**$_2$-, from DLD), 3.68 (**a`**) (-C**H**$_2$-OH, end group from 1,4-BDO), 2.33 (**c,d**) (4H, -CO-C**H**$_2$-, from DA), 1.71 (4H, -O-CH$_2$-C**H**$_2$-, from 1,4-BDO), 1.66 (**f**) (4H, -CO-CH2-C**H**$_2$-, from DA), 1.26 (**g,i,j,k**) (-C**H**$_2$-, from DLD), 0.88 (**h**) (6H, -CH2-C**H**$_3$, end group of DLD). Based on ^{1}H NMR analysis the expected chemical structure of PBA-DLA was established. This is evidenced by the presence of signals (a) and (e), which clearly indicate the formation of ester bonds, and also the presence of the (f), (g), (h), (i), (j), (k) signals which confirms that the long chain of dilinoleic diol has been successfully incorporated into the copolymer chain.

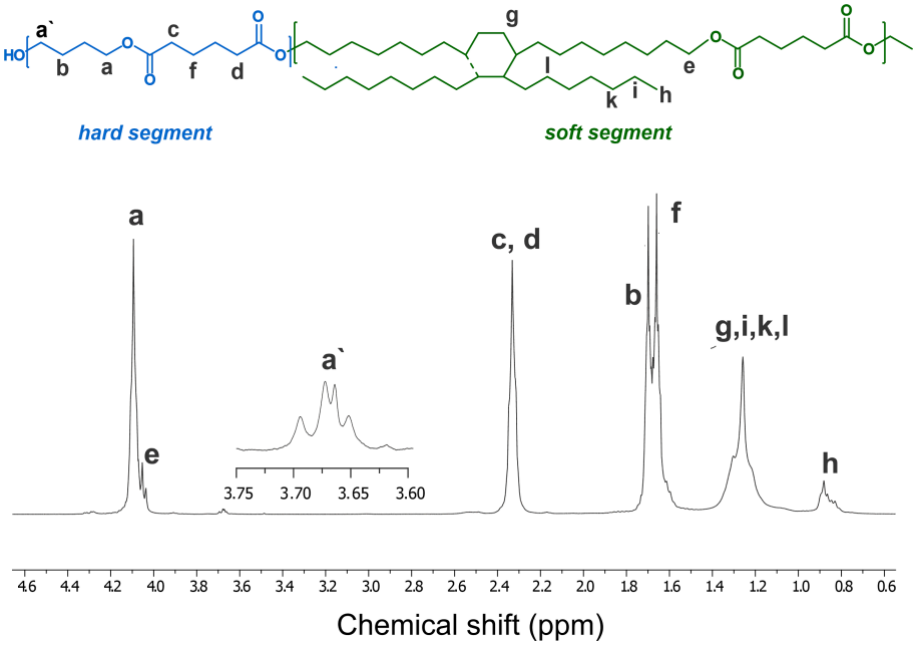

Figure 3. ^{1}H NMR spectra of PBA-DLA copolymer

Moreover, based on the values of integrals of signals characteristic for hard and soft segments, a more detailed analysis was performed, on the basis of which the real ratio of hard to soft segments and number average molecular weight (M_n) were calculated following the method described in our previous work [25]. According to data presented in Table 1, PBA-DLA is characterized by relatively high molecular weight, however, the calculated hard to soft segment ratio differs from values estimated theoretically, which may be related to the evaporation of 1,4-butanediol at the synthesis stage when the high vacuum was applied.

Table 1. The composition of PBA-DLA copolyester determined from ^{1}H NMR

Copolymer	**Composition**		**^{1}H NMR**
	Theoretical wt% [mol%]	Calculated wt% [mol%]	M_n [g/mol]
PBA-DLA	70-30 [88.4-11.6]	63.3-36.7 [84.9-15.1]	15 900

Due to the potential application of copolymer as a drug delivery system (contact with the body), it was extremely important to verify material biocompatibility. Therefore, to assess any cytotoxic or growth-inhibitory effect of the PBA-DLA copolyester, an *in vitro* indirect contact assay was performed using L929 murine fibroblasts. Cells were incubated in the presence of extract from reference (PCL) and PBA-DLA samples for 24 h and viability was

measured using an inverted light microscope and resazurin viability assay. After 24 hours of culture, a clear negative effect of PCL and PBA-DLA material was observed (Figure 4). No toxic contaminants were present as proved by the robust growth and typical flattened cell morphology after incubation in extracts from control, reference, and tested materials. The microscopic observations were also supported by the results of the resazurin viability assay based on which normalized viability was calculated. Obtained values are in good agreement with visual evaluation. L929 doubling time is typically approx. 20-22 hours, thus cell viability values below 70% indicate cytotoxicity. The average values of normalized cells viability (CV%) obtained for PCL and PBA-DLA were 98 $\pm$ 6 and 91 $\pm$ 5 %, respectively.

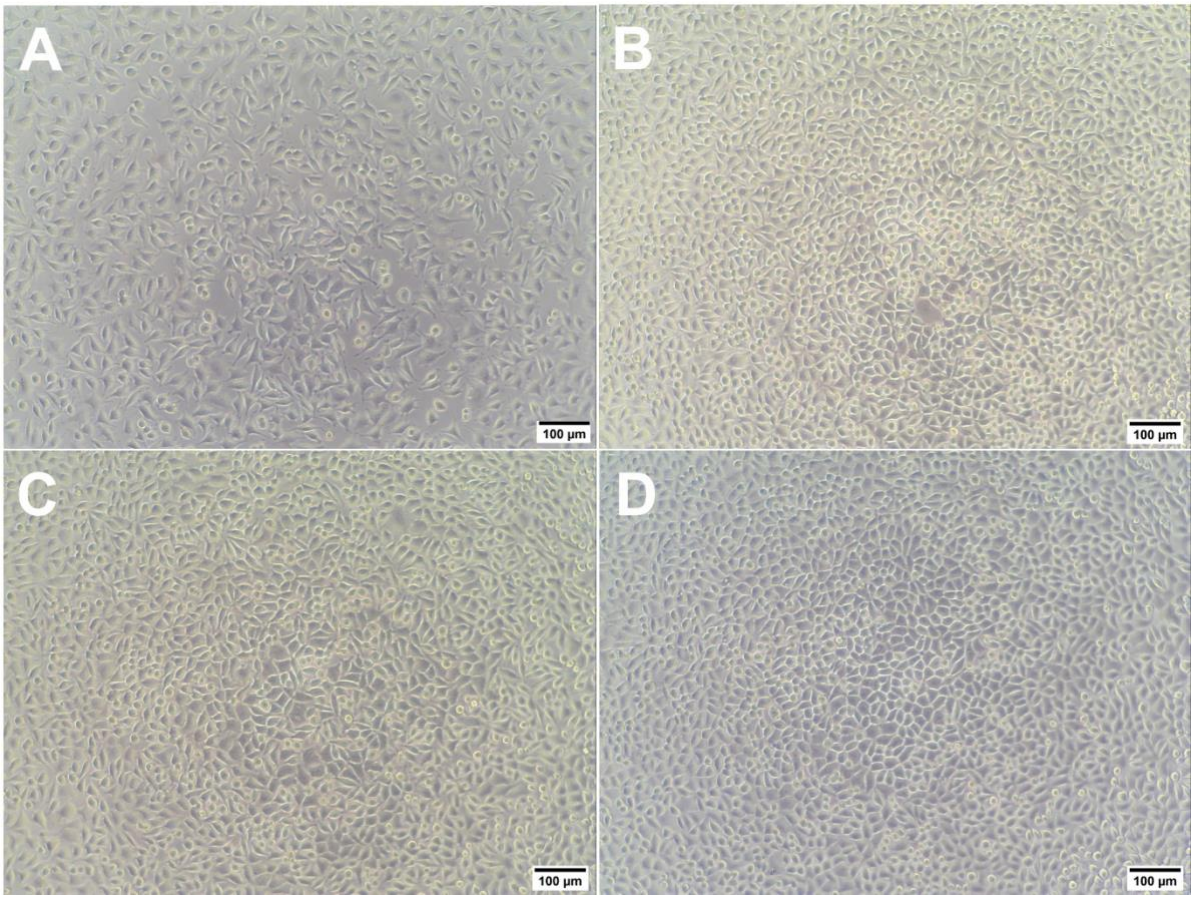

Figure 4. Representative micrographs of L929 cells seeded at 10000 cells per well. A) Cells 24 hours after seeding. B) Cells further 24 hours of culture without extracts. Cells cultured for 24 hours with extracts from C) reference material (PCL sample) and D) tested PBA-DLA material.

After receiving positive results from the cytotoxicity assessment, the manufacturing of PBA-DLA nanoparticles (NPs) *via* the nanoprecipitation method has been started. In this work, acetone was chosen as the solvent since it is widely used in the manufacturing of PNPs *via* nanoprecipitation, mainly due to the safety aspects, easy evaporation, and good miscibility with

water (expressed by Hildebrand solubility parameter) which should be considered while performing nanoprecipitation since interactions between molecules of water and organic solvent are influencing polymer NPs size [26]. According to the values obtained from DLS measurements presented in Table 2 and Figure 5 it was possible to obtain stabilizer-free NPs with a hydrodynamic diameter (HD) of 201.9 ± 0.2 characterized by a low dispersity index (DI). However, during the purification (centrifugation) step, problems related to the redispersion of NPs were encountered as evidenced by the size of NPs (421.9 ± 7.4) and significantly higher DI (0.282 ± 0.066). Part of the NPs also deposited and agglomerated on the walls of the vial and therefore, it was decided to use Pluronic F127 (PLUR) as a stabilizer in order to eliminate this drawback. Stabilizer used in the concentrations of 0.05 and 0.1 mg/ml allowed to obtain NPs with HD of 149.1 ± 0.4 and 190.2 ± 2.5, respectively, and DI of 0.017 ± 0.013 and 0.018 ± 0.010, respectively. Additionally, in both cases, it was possible to fully redisperse the NPs after purification steps, as evidenced by the comparable HD values and low DI (see Table 2). Interestingly enough, it was clearly confirmed that the smallest NPs diameter (149.1 ± 0.4) is obtained at 0.05 mg/ml of PLUR concentration. Increase in the PLUR concentration to 0.1 mg/ml resulted in higher NPs size (190.2 ± 2.5) and most probably this is related to the fact, that higher PLUR concentration changed the aqueous solution parameters, affecting the reduced miscibility of the acetone phase with the aqueous phase and as a result particles with higher size were formed.

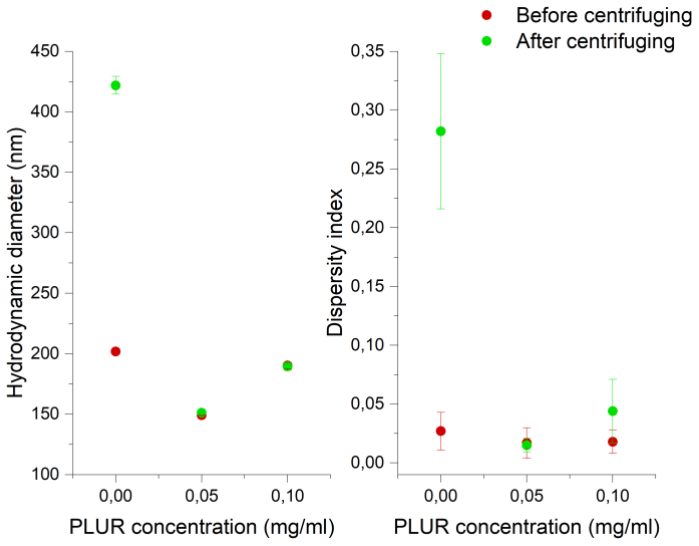

Figure 5. Effect of PLUR stabilizer concentration (Pluronic F127) on PBA-DLA NPs size and dispersity index.

Table 2. The PBA-DLA nanoparticles the average hydrodynamic diameter (HD) and dispersity index (DI) measured by DLS.

Acetone phase	Aqueous phase	Before purification		After purification	
$c_{PBA-DLA}$ (mg/ml)	c_{PLUR} (mg/ml)	HD (nm)	DI	HD (nm)	DI
10	0	201.9 ± 0.2	0.027 ± 0.016	421.9 ± 7.4	0.282 ± 0.066
	0.05	149.1 ± 0.4	0.017 ± 0.013	151.3 ± 0.5	0.015 ± 0.006
	0.1	190.2 ± 2.5	0.018 ± 0.010	189.5 ± 3.3	0.044 ± 0.027

Once the neat PBA-DLA NPs manufacturing process was optimized, work connected with α-tocopherol (α-TP) encapsulation started. In order to determine the role of α-TP amount on the NPs size and encapsulation efficiency, three different concentrations of α-TP were tested (2.5, 5, and 10 mg/ml). The average particle diameters and DI values were measured by DLS, and the results were summarized in Table 3. According to the collected data, the diameter of NPs permanently increases with increasing α-TP concentration (from 145.5 to 176.3 nm) (Figures 6 and 7). This phenomenon may be related to the fact that part of α-TP is encapsulated in the core of PBA-DLA NPs, while the remaining part is located on the surface of the polymer shell. The increasing amount of α-TP in the acetone phase led to the NPs formation with a higher amount of the drug located on the surface, thus, NPs with higher diameter were formed. Our speculations should be additionally supported by microscopic observations to prove that, however, similar research were carried out by Varga *et al.* [11] in which they performed α-TP encapsulation using poly(lactide acid) (PLA) which similarly to PBA-DLA copolymer possess hydrophobic character. In the cited work, PLA NPs with α-TP were obtained *via* nanoprecipitation method where transmission electron microscopy (TEM) images were recorded showing that α-TP is located in the core of the NPs and on the surface.

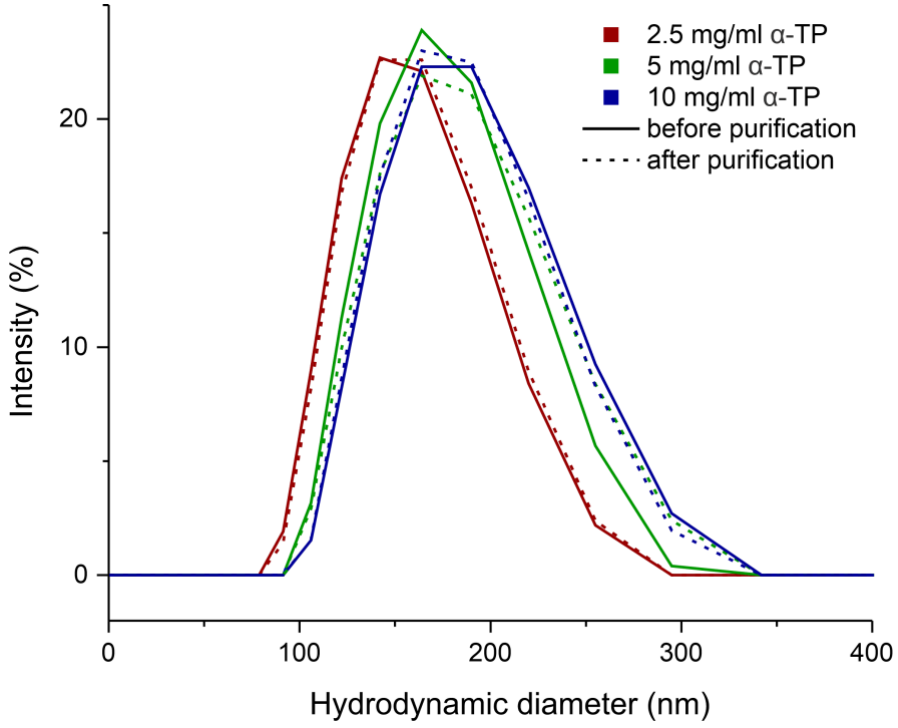

Figure 6. PBA-DLA nanoparticles size distribution.

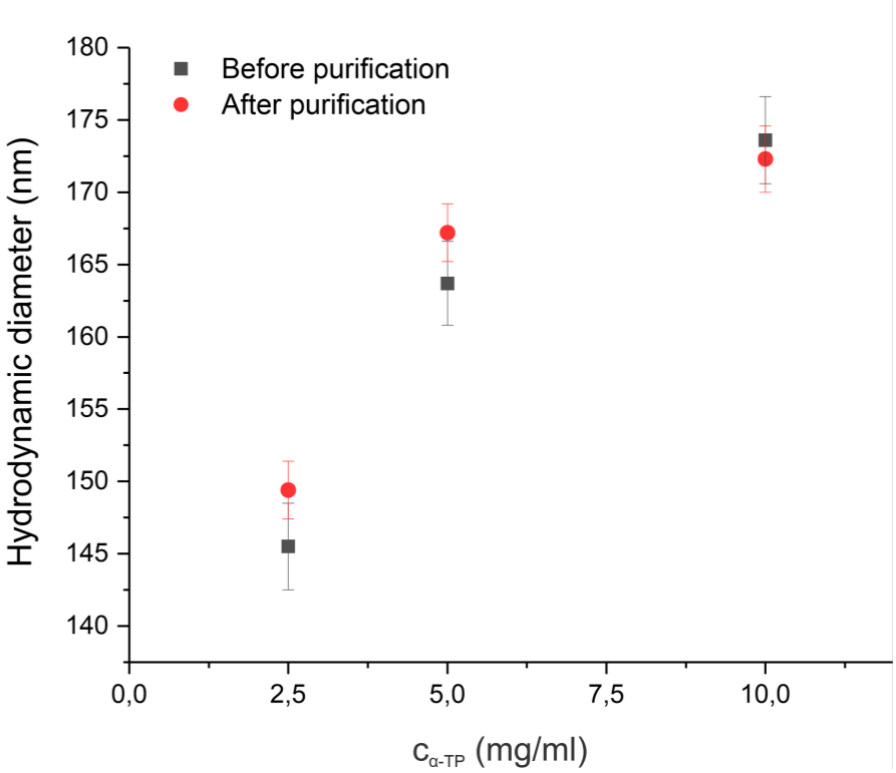

Figure 7. PBA-DLA NPs size distribution depending on α-TP concentration.

Table 3 Components concentration, the average hydrodynamic diameter (HD) and dispersity index (DI) of particles before and after purification step and the encapsulation efficiency (EE%)

Acetone phase		Aqueous phase	Before purification		After purification		
$c_{PBA-DLA}$ (mg/ml)	$c_{\alpha-TP}$ (mg/ml)	c_{PLUR} (mg/ml)	HD (nm)	DI	HD (nm)	DI	EE (%)
10	2.5	0.05	145.5 ± 3.0	0.044 ± 0.008	149.4 ± 2.0	0.025 ± 0.017	48
	5		163.7 ± 2.9	0.032 ± 0.009	167.2 ± 2.0	0.048 ± 0.027	74
	10		176.3 ± 3.0	0.052 ± 0.025	172.3 ± 2.3	0.023 ± 0.020	50

After the characterization of the α-TP size, encapsulation efficiency (EE%) was assessed based on the calibration curve prepared using UV-VIS spectroscopy (Figure 8). Performed studies indicate that by using α-TP concentration of 5 mg/ml we were able to obtain the highest encapsulation efficiency (74 %) whereas in case of 2.5 and 10 mg/ml those value was calculated to be 50 %.

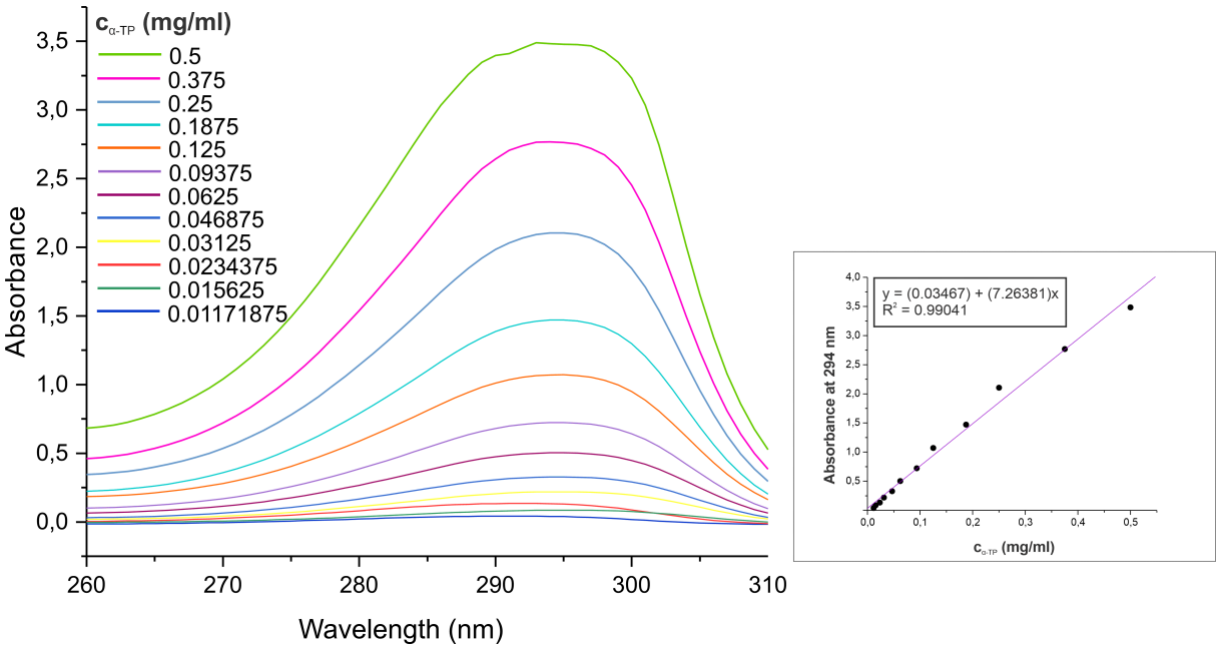

Figure 8. UV-VIS spectra of α-TP in different concentrations dissolved in 1,4-dioxane containing PBA-DLA (10 mg/ml)

Furthermore, the α-TP-loaded NPs have been additionally examined by ^{1}H NMR measurements. Figure 9 depicts the spectra of the neat PBA-DLA and PBA-DLA-based NPs in the presence of α-TP used at different concentrations (2.5, 5, 10 mg/ml). The detailed NMR assignments are as follows: ^{1}H NMR (400 MHz, $CDCl_3$-d_1, ppm): 4.27 (**f**) (H, C-O**H**), 2.60 (b) (2H, -O-C-CH_2-C**H**$_2$-), 2.16 (**c**) (HO-C-C-C**H**$_3$), 2.11 (**a**) (6H, -C-C-C**H**$_3$), 1.76 (**h**) (2H, -O-C-

C**H**$_2$-), 1.23 (**d**) (3H, -O-C-C**H**$_3$), 1.13 (**i**) (2H, -C**H**$_2$-CH-CH$_3$), 1.06 (**j**) (4H, C**H**$_2$-C-CH$_3$), 0.86 (**e,g**) (12H, -C**H**$_3$). Based on ^{1}H NMR analysis the presence of α-TP within PBA-DLA NPs was confirmed as evidenced by the presence of above mentioned signals. Notably, increased signals intensities can be observed for sample where 5 mg/ml of α-TP concentration was applied during NPs preparation which is an line with calculated EE% values.

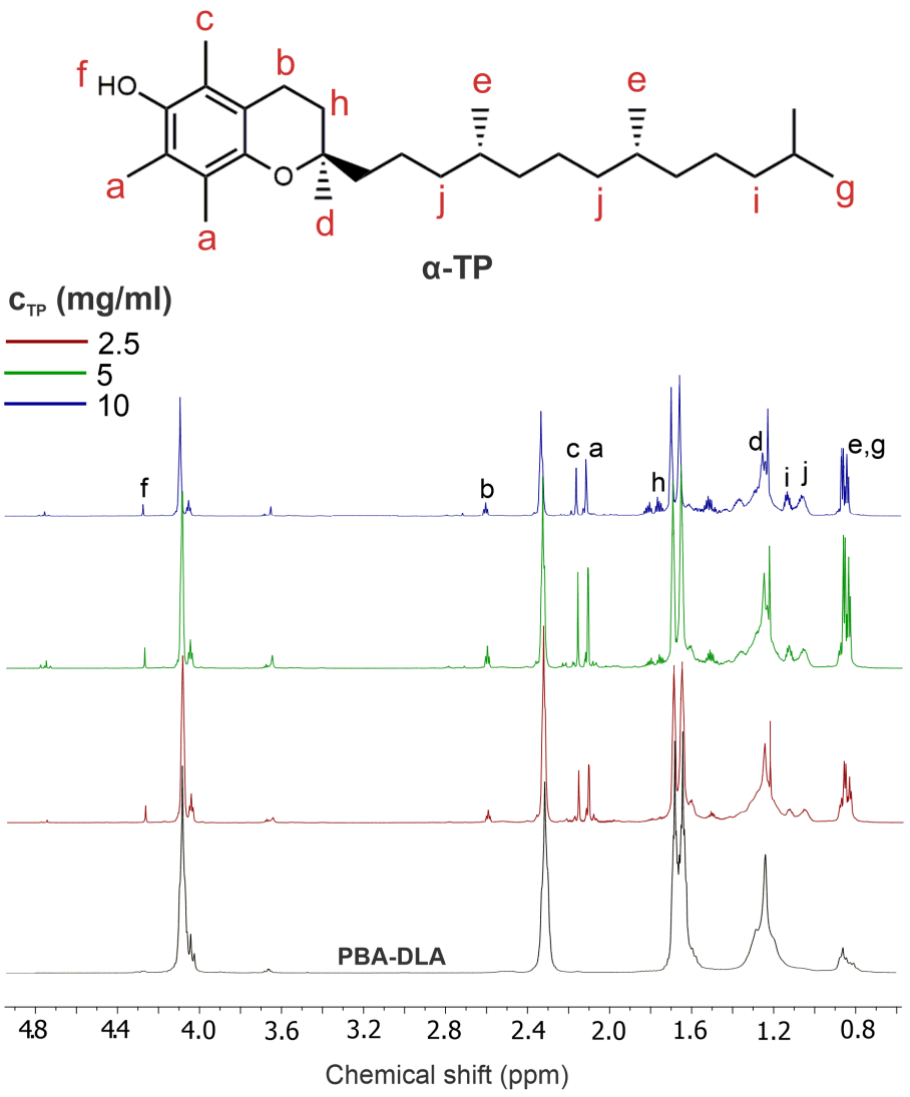

Figure 6 ^{1}H NMR spectra of PBA-DLA NPs containing different concentrations of α-TP after purification and lyophilization.

4. Conclusions

PBA-DLA copolymer was enzymatically synthesized using CALB as a biocatalyst and its chemical structure and potential usage in the biomedical field were evaluated. Performed work indicated on successful encapsulation of hydrophobic α-tocopherol - one of the determinative

forms of vitamin E, using novel biocompatible PBA-DLA copolyester. The NPs were prepared by nanoprecipitation method and DLS measurements showed that by using neat PBA-DLA (without α-TP and stabilizer) it is possible to produce narrowly distributed particles with a particle size of ~202 nm, however, NPs tend to agglomerate during purification (centrifugation) step and therefore PLUR stabilizer was used to eliminate this drawback. Optimization of the experimental conditions, mainly the concentration of PLUR stabilizer resulted in the formation of α-TP-loaded NPs within the hydrodynamic diameter range of ~146-176 nm. NPs size was increasing with higher α-TP concentration which according to our speculations is related to the higher amount of active ingredient located on the surface of the polymer shell. Furthermore, based on the calibration curve prepared using UV-VIS spectroscopy, the α-TP encapsulation efficiency (EE%) was calculated. Performed studies indicated that the highest EE% values were reached by using α-TP concentration of 5 mg/ml (74 %) whereas in case of 2.5 and 10 mg/ml EE% was calculated to be ~50 %. Finally, ^{1}H NMR measurements were performed for neat PBA-DLA and NPs obtained using different concentrations of α-TP. Recorded spectra confirmed the presence of α-TP and indicate that intensities of signals characteristic for α-TP are increased for NPs produced using 5 mg/ml of α-TP which is consistent with EE% values calculated for α-TP-based NPs. Performed work proved that PBA-DLA copolymers are potential candidates for drug delivery systems and encapsulation of hydrophobic α-TP.

Author Contributions: Conceptualization, M.S and M.E.F; methodology, M.S, M.M, M.E.F; validation, M.S., M.M., M.E.F.; formal analysis, M.E.F.; investigation, M.S., M.M., M.E.F; writing—original draft preparation, M.S.; writing—review and editing, M.E.F.; visualization, M.S; supervision, M.E.F.

Funding: This project has received funding from the European Union's Horizon 2020 research and innovation program under the Marie Skłodowska-Curie grant agreement no. 872152

Acknowledgments: The authors acknowledge funding from the European Union's Horizon 2020 research and innovation program under Marie Skłodowska-Curie grant agreement no. 872152 (GREEN-MAP). Scientific work published as part of an international project co-financed by the program of the Minister of Science and Higher Education entitled "PMW" in the years 2000-2023; contract No. 5091/H2020/2020/2.

Conflicts of Interest: The authors declare no conflict of interest.

5. References

[1] Peer D, Karp JM, Hong S, Farokhzad OC, Margalit R, Langer R. Nanocarriers as an emerging platform for cancer therapy. Nat Nanotechnol 2007;2:751–60. https://doi.org/10.1038/nnano.2007.387.

[2] Castaldello A, Brocca-Cofano E, Voltan R, Triulzi C, Altavilla G, Laus M, et al. DNA prime and protein boost immunization with innovative polymeric cationic core-shell nanoparticles elicits broad immune responses and strongly enhance cellular responses of HIV-1 tat DNA vaccination. Vaccine 2006;24:5655–69. https://doi.org/10.1016/j.vaccine.2006.05.058.

[3] Houchin-Ray T, Whittlesey KJ, Shea LD. Spatially Patterned Gene Delivery for Localized Neuron Survival and Neurite Extension. Molecular Therapy 2007;15:705–12. https://doi.org/10.1038/sj.mt.6300106.

[4] Sun W, Wang H, Xie C, Hu Y, Yang X, Xu H. An attempt to directly trace polymeric nanoparticles in vivo with electron microscopy. Journal of Controlled Release 2006;115:259–65. https://doi.org/10.1016/j.jconrel.2006.08.007.

[5] Mohd Zaffarin AS, Ng S-F, Ng MH, Hassan H, Alias E. Pharmacology and Pharmacokinetics of Vitamin E: Nanoformulations to Enhance Bioavailability. Int J Nanomedicine 2020;Volume 15:9961–74. https://doi.org/10.2147/IJN.S276355.

[6] Kamaly N, Xiao Z, Valencia PM, Radovic-Moreno AF, Farokhzad OC. Targeted polymeric therapeutic nanoparticles: design, development and clinical translation. Chem Soc Rev 2012;41:2971. https://doi.org/10.1039/c2cs15344k.

[7] Zhang L, Chan JM, Gu FX, Rhee J-W, Wang AZ, Radovic-Moreno AF, et al. Self-Assembled Lipid−Polymer Hybrid Nanoparticles: A Robust Drug Delivery Platform. ACS Nano 2008;2:1696–702. https://doi.org/10.1021/nn800275r.

[8] Chou LYT, Ming K, Chan WCW. Strategies for the intracellular delivery of nanoparticles. Chem Soc Rev 2011;40:233–45. https://doi.org/10.1039/C0CS00003E.

[9] Lassalle V, Ferreira ML. PLA Nano- and Microparticles for Drug Delivery: An Overview of the Methods of Preparation. Macromol Biosci 2007;7:767–83. https://doi.org/10.1002/mabi.200700022.

[10] Jiang X, Xin H, Ren Q, Gu J, Zhu L, Du F, et al. Nanoparticles of 2-deoxy-d-glucose functionalized poly(ethylene glycol)-co-poly(trimethylene carbonate) for dual-targeted drug delivery in glioma treatment. Biomaterials 2014;35:518–29. https://doi.org/10.1016/j.biomaterials.2013.09.094.

[11] Varga N, Turcsányi Á, Hornok V, Csapó E. Vitamin E-Loaded PLA- and PLGA-Based Core-Shell Nanoparticles: Synthesis, Structure Optimization and Controlled Drug Release. Pharmaceutics 2019;11:357. https://doi.org/10.3390/pharmaceutics11070357.

[12] McCall RL, Sirianni RW. PLGA Nanoparticles Formed by Single- or Double-emulsion with Vitamin E-TPGS. Journal of Visualized Experiments 2013. https://doi.org/10.3791/51015.

[13] Park K, Skidmore S, Hadar J, Garner J, Park H, Otte A, et al. Injectable, long-acting PLGA formulations: Analyzing PLGA and understanding microparticle formation. Journal of Controlled Release 2019;304:125–34. https://doi.org/10.1016/j.jconrel.2019.05.003.

[14] Wan F, Yang M. Design of PLGA-based depot delivery systems for biopharmaceuticals prepared by spray drying. Int J Pharm 2016;498:82–95. https://doi.org/10.1016/j.ijpharm.2015.12.025.

[15] Ecoflex® (PBAT): The original since 1998 – certified compostable biopolymer n.d. https://plastics-rubber.basf.com/global/en/performance_polymers/products/ecoflex.html (accessed November 10, 2022).

[16] Siafaka PI, Barmbalexis P, Bikiaris DN. Novel electrospun nanofibrous matrices prepared from poly(lactic acid)/poly(butylene adipate) blends for controlled release formulations of an anti-rheumatoid agent. European Journal of Pharmaceutical Sciences 2016;88:12–25. https://doi.org/10.1016/j.ejps.2016.03.021.

[17] Koster RM, Bogert M, de Leeuw B, Poels EK, Bliek A. Active sites in the clay catalysed dimerisation of oleic acid. J Mol Catal A Chem 1998;134:159–69. https://doi.org/10.1016/S1381-1169(98)00032-6.

[18] Jäger A, Gromadzki D, Jäger E, Giacomelli FC, Kozlowska A, Kobera L, et al. Novel "soft" biodegradable nanoparticles prepared from aliphatic based monomers as a potential drug delivery system. Soft Matter 2012;8:4343. https://doi.org/10.1039/c2sm07247e.

[19] Prowans P, Kowalczyk R, Wiszniewska B, Czapla N, Bargiel P, El Fray M. Bone Healing in the Presence of a Biodegradable PBS-DLA Copolyester and Its Composite Containing Hydroxyapatite. ACS Omega 2019;4:19765–71. https://doi.org/10.1021/acsomega.9b02539.

[20] Skrobot J, Zair L, Ostrowski M, el Fray M. New injectable elastomeric biomaterials for hernia repair and their biocompatibility. Biomaterials 2016;75:182–92. https://doi.org/10.1016/j.biomaterials.2015.10.037.

[21] Tallawi M, Zebrowski DC, Rai R, Roether JA, Schubert DW, el Fray M, et al. Poly(Glycerol Sebacate)/Poly(Butylene Succinate-Butylene Dilinoleate) Fibrous Scaffolds for Cardiac Tissue Engineering. Tissue Eng Part C Methods 2015;21:585–96. https://doi.org/10.1089/ten.tec.2014.0445.

[22] Bahramian B, Ma Y, Rohanizadeh R, Chrzanowski W, Dehghani F. A new solution for removing metal-based catalyst residues from a biodegradable polymer. Green Chemistry 2016;18:3740–8. https://doi.org/10.1039/C5GC01687H.

[23] Riss TL, Moravec RA. Use of Multiple Assay Endpoints to Investigate the Effects of Incubation Time, Dose of Toxin, and Plating Density in Cell-Based Cytotoxicity Assays. Assay Drug Dev Technol 2004;2:51–62. https://doi.org/10.1089/154065804322966315.

[24] Ciecholewska-Juśko D, Żywicka A, Junka A, Drozd R, Sobolewski P, Migdał P, et al. Superabsorbent crosslinked bacterial cellulose biomaterials for chronic wound dressings. Carbohydr Polym 2021;253:117247. https://doi.org/10.1016/j.carbpol.2020.117247.

[25] Sokołowska M, Nowak-Grzebyta J, Stachowska E, El Fray M. Enzymatic Catalysis in Favor of Blocky Structure and Higher Crystallinity of Poly(Butylene Succinate)-Co-(Dilinoleic Succinate) (PBS-DLS) Copolymers of Variable Segmental Composition. Materials 2022;15:1132. https://doi.org/10.3390/ma15031132.

[26] de Oliveira AM, Jäger E, Jäger A, Stepánek P, Giacomelli FC. Physicochemical aspects behind the size of biodegradable polymeric nanoparticles: A step forward. Colloids Surf A Physicochem Eng Asp 2013;436:1092–102. https://doi.org/10.1016/j.colsurfa.2013.08.056.